Novel ultrafast laser ablation by biburst in MHz and GHz pulse repetition rate

Andrius Žemaitis[1]*, Mantas Gaidys[1], Paulius Gečys[1], Martynas Barkauskas[2], Mindaugas Gedvilas[1]

[1] Department of Laser Technologies (LTS), Center for Physical Sciences and Technology (FTMC), Savanoriu Ave. 231, 02300 Vilnius, Lithuania

[2] Light Conversion Ltd., Keramiku st. 2B, 10233 Vilnius, Lithuania

Correspondence and requests for materials should be addressed to A.Ž. (E-mail: andrius.zemaitis@ftmc.lt).

Abstract

Here, to the best of our knowledge, for the first time we report the in-depth study of extremely high ultrafast laser ablation efficiency for processing of copper and steel with single-pulses, MHz-, GHz- and burst in the burst (biburst) regime. The comparison of burst, biburst and single-pulse ablation efficiencies was performed for beam-size-optimised regimes, showing the real advantages and disadvantages of milling and drilling processing approaches. Highly-efficient ultrashort pulse laser processing was achieved for ~1 µm wavelength: 8.8 $\mu m^3/\mu J$ for copper drilling, 5.6 $\mu m^3/\mu J$ for copper milling, and 6.9 $\mu m^3/\mu J$ for steel milling. We believe that the huge experimental data collected in this study will serve well for the better understanding of laser burst-matter interaction and theoretical modelling.

Keywords

Ultrafast laser; burst; biburst; milling; drilling; ablation efficiency; GHz burst

1. Introduction

To fulfil a high throughput and quality requirements coming from the laser-based manufacturing industry, laser technology must constantly evolve. Therefore, laser source manufacturers build lasers with hundreds of watts of average optical power, pulse repetition rates in the range of MHz and even GHz and near-THz in the burst mode regimes [1,2]. Newly developed fast laser beam scanning systems are capable of reaching scanning speeds of hundreds of meters per second [3]. All the effort is dedicated to make faster laser manufacturing and to keep the laser technology the number one choice for precise material processing. Ultrafast lasers are high-tech products which still hold a high price for know-how and technology, therefore each laser produced photon is very expensive. For example, ultrafast laser source with an average optical power of tens of watts could easily reach the price of €100k. For this reason, it is extremely important to use laser energy in the most efficient way possible. In the pursuit of higher processing efficiency, the laser sources with burst mode capability were created. These lasers generate packages of pulses called bursts with intra-burst pulse repetition rates up to GHz range. For the conventional, single-pulse laser working regime, it is known that the ablation process indeed can benefit from the high pulse repetition rate as it induces heat

accumulation [4]. For the subsequent pulses the sample is pre-heated due to heat accumulation and the energy required to evaporate the material is lower [5]. In the case of low repetition rate, the generated thermal energy has enough time between pulses to spread over the sample and surrounding environment. Therefore, heat induced by every previous laser pulse is lost and not beneficial for the ablation process. For GHz burst the mechanism of material removal via ablation-cooled process was discussed, which claimed ablation efficiency increase due to the removal of excess thermal energy from the material with the successive pulses [6]. Comparison of single-pulse versus burst mode processing has to be done carefully, since both regimes have to be optimised beforehand and only then compared [7]. In the case of manufacturing processes based on laser ablation such as milling, cutting or drilling, the optimisation of ablation efficiency can be done by varying the laser fluence [8,9]. This optimisation allows to find the most efficient working point, where the highest volume of the material can be removed per unit of energy or/and time. Also, the processing approach has to be taken into account when comparing ablation efficiencies, as different processes might happen during laser drilling and milling as heat accumulation, melt formation and repulsion of melt out of the processing area.

Here, for the first time we demonstrate the in-depth study of ultrafast laser ablation by biburst of metals (copper and stainless steel). The biburst laser technology generates burst-in-burst: the package of laser pulses with GHz repetition rate are repeated again at tens of MHz repetition rate burst. The comparison of single-pulse with burst regime in MHz, GHz and biburst was conducted for the drilling and milling processing approaches. In the case of copper MHz burst processing a strong influence of odd and even number of pulses within the burst was measured for both drilling and milling. Due to the beam-size-optimisation the highest milling ablation efficiencies were measured of 5.6 $\mu m^3/\mu J$ and 6.9 $\mu m^3/\mu J$ for copper and stainless steel, respectively. At GHz burst processing a big decrease of ablation efficiency was measured for both tested metals. Contrary to GHz burst, the biburst processing demonstrated the high ablation efficiency of 8.4 $\mu m^3/\mu J$ for copper drilling, which was higher than single-pulse drilling efficiency. Contrary, laser milling approach by biburst had a lower ablation efficiency than a single-pulse and MHz burst processing modes for both tested metals. In addition, we believe, that the huge experimental data collected in this study will serve well for the better understanding of laser burst-matter interaction and theoretical modelling [10–13].

2. Materials and methods

2.1. Experimental setup

A solid-state laser (Pharos, Light Conversion) capable of producing light pulses of $\tau = 210$ fs duration at $\lambda = 1030$ nm wavelength was used in the experiments. The state-of-the-art laser had 4 working regimes: 1) the conventional single-pulse regime – emitting one pulse every $\Delta t_P = 10$ µs which corresponds to a pulse repetition rate of $f_P = 100$ kHz (Fig. 1 a), 2) MHz burst – emitting burst of pulses with an intra-burst repetition

rate of f_{MHz} = 64.68 MHz (Δt_P = 15.45 ns) with the number of pulses within the burst ranging from N = 2 to N = 9 (Fig. 1 b), 3) GHz burst – emitting burst of pulses with an intra-burst repetition rate of f_{GHz} = 4.88 GHz, (Δt_P = 205 ps) with the number of pulses within the burst ranging from P = 2 to P = 25 (Fig. 1 c), 4) Biburst – burst in the burst regime, where a set of 4.88 GHz burst pulses can be burst again at 64.5 MHz (Fig. 1 d). The laser was always working at a burst (or biburst) repetition rate of f_B = 100 kHz during any of the burst scenarios. For biburst all combinations of N and P values were possible. A maximum average optical power on the sample surface was P_{ave} = 7.3 W, which was always kept constant during the experiments.

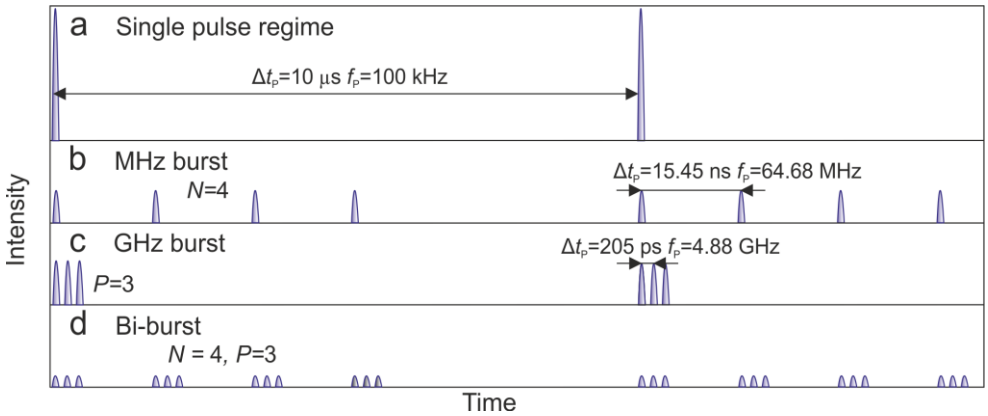

Fig. 1. Illustration of four possible laser working regimes: (a) Single-pulse regime with a pulse repetition rate of f_P = 100 kHz; (b) N = 4-pulse MHz burst with an intra-burst repetition rate of f_{MHz} = 64.68 MHz and a burst repetition rate of f_B = 100 kHz; (c) P = 3-pulse GHz burst with an intra-burst repetition rate of f_{GHz} = 4.88 GHz and a burst repetition rate of f_B = 100 kHz; (d) Biburst regime with an intra-burst repetition rate of f_{GHz} = 4.88 GHz with P = 3 pulses within a burst and a burst repetition rate of f_{MHz} = 64.68 MHz with N = 4 bursts within the biburst and a biburst repetition rate of f_B = 100 kHz.

A galvanometer scanner (Intelliscan 14, Scanlab) together with a F-theta lens with a focal distance of 100 mm were used to scan and focus the laser beam. Laser beam radii w along z vertical position were measured by the D-squared technique [14]. This technique allows to determine w due to the laser-induced damage diameter D dependence on irradiated pulse energy E_p:

$$D^2 = 2w^2 \ln\left(\frac{E_p}{E_{th}}\right), \tag{1}$$

where E_{th} – damage threshold energy. By fitting the experimental data using Equation (1), the beam radii w at different z positions were extracted from the slope of the linear function (Fig. 2 a). The gaussian beam divergence equation was used to fit data obtained by the D-squared technique (Fig. 2 b) [15]:

$$w(z) = w_0 \sqrt{1 + \left(\frac{(z - z_0)\lambda M^2}{\pi w_0^2}\right)^2}, \tag{2}$$

where w_0 – beam radius at waist, z_0 – beam waist position, λ = 1030 nm – laser wavelength, M^2 – beam quality factor. The retrieved parameters were: beam radius at focus w_0 = 19.6 ± 0.4 µm and quality factor M^2 = 1.07 ± 0.03. The Rayleigh length was approximately z_R = 1.1 mm.

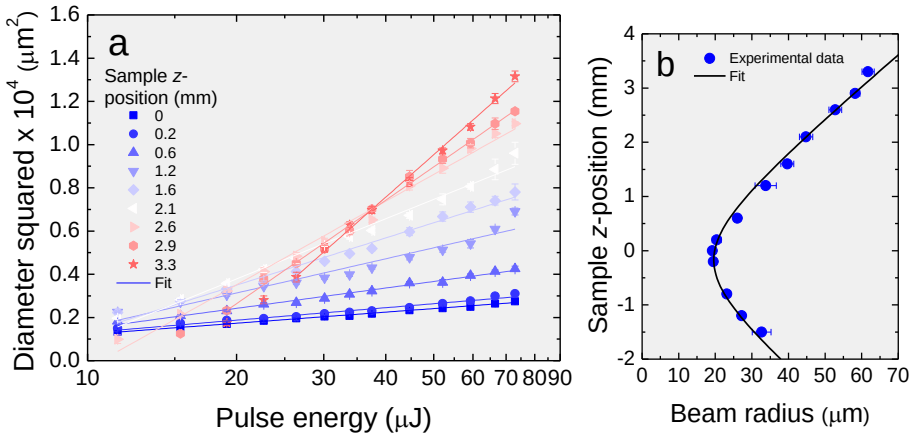

Fig. 2. Gaussian beam characterisation. (a) Beam radius measurement at different *z* sample vertical positions by the *D*-squared method. Experimental data fitted by laser damage diameter – pulse energy Equation (1). (b) Gaussian beam waist calculation by data extracted from the *D*-squared method. Data fitted by the Gaussian beam divergence Equation (2).

2.2. Experiment design

Laser ablation efficiencies of metal samples were measured by two approaches: 1) ablation of craters – percussion drilling also known as laser punching with fixed beam position, 2) ablation of rectangular cavities – milling by scanned laser beam. In both approaches for one set of laser processing parameters the maximum ablation efficiency was investigated by changing the beam size from w = 21 µm at a position close to z_0 focal position to w = 95 µm at Δz = 5.3 mm out of focus. By increasing the distance between focusing lens and sample surface, the beam size w was increased and therefore the peak pulse fluence F_0 was varied:

$$F_0 = \frac{2P_{\mathrm{ave}}}{f_{\mathrm{P,B}} \cdot \pi w^2(z) NP}, \tag{3}$$

where P_{ave} = 7.3 W and $f_{\mathrm{P,B}}$ = 100 kHz – average optical power and repetition rate which were always kept constant during the experiments, $w(z)$ – beam radius at z position according to Equation (1), N and P – pulse number within MHz burst and GHz burst, respectively. The ablation efficiencies versus pulse fluence were measured in MHz burst regime for pulses per burst N = 2, 3, 4, 5, 6, 7, 8, 9, in GHz burst regime for pulses per burst P = 2, 3, 4, 5, 6, 7, 8, 9, 10, 15, 20, 25 and in biburst regime all N and P combinations. Also, the ablation efficiency versus pulse fluence was measured for a single-pulse regime to have a comparison between the conventional single-pulse and burst regimes. In total 1287 (11 beam radii, single-pulse regime, 8 number of pulses per MHz burst, 12 number of pulses per GHz burst and 8 × 12 =96 combinations for biburst) craters and 1287 rectangular cavities were ablated and measured for copper sample and 1287 rectangular cavities for stainless steel sample.

2.2.1. Laser drilling

Each of the crater was ablated by m = 10 bursts on one spot to have a higher depth and volume for more reliable data and a situation closer to real percussion drilling process by multiple shots. The highest depth of the crater was not higher than 20 µm, which was in linear depth dependence on pulse number on one spot and very far away from crater depth saturation case [16]. Volumes V of the ablated craters were measured by 3D optical profiler (S neox, Sensofar) (Fig. 3 a). The ablation efficiency was calculated dividing the measured volume V by the total accumulated energy on one spot $E_{ACC} = m \cdot P_{ave}/f_{P,B}$= 730 µJ which was always constant during the experiments.

2.2.2. Laser milling

Rectangular cavities with dimensions of 2 mm × 1 mm = 2 mm^2 were engraved into the metal samples. The rectangles were filled with pattern of parallel lines separated by Δy = 10 µm hatch distance. Beam scanning speed of v = 333 mm/s was used, resulting in $\Delta x = v/f_B \approx$ 3.3 µm spot-to-spot or pitch distance. The rectangles were scanned multiple times n to increase the depths of the cavities for more reliable data and to have a process closer to the industrial laser milling case with multiple layer scan. Typical depths of the cavities were in the range of tens of micrometres. Therefore, the defocusing of laser beam inside the cavity after the layer scan was negligible since Rayleigh length was close to one millimetre. The depth of the cavity and surface roughness R_a were measured by the stylus profiler Dektak 150+ (Veeko) (Fig. 3 b, c). Ablation efficiency η_E for every set of processing parameters was calculated from the cavity depth h:

$$\eta_{\mathrm{E}} = \frac{V}{E_{\mathrm{ACC}}} = \frac{\Delta y v h}{P_{\mathrm{ave}} n}, \tag{4}$$

where Δy = 10 µm – hatch distance, v = 333 mm/s – beam scanning speed, P_{ave} = 7.3 W – average optical power and n – number of scans.

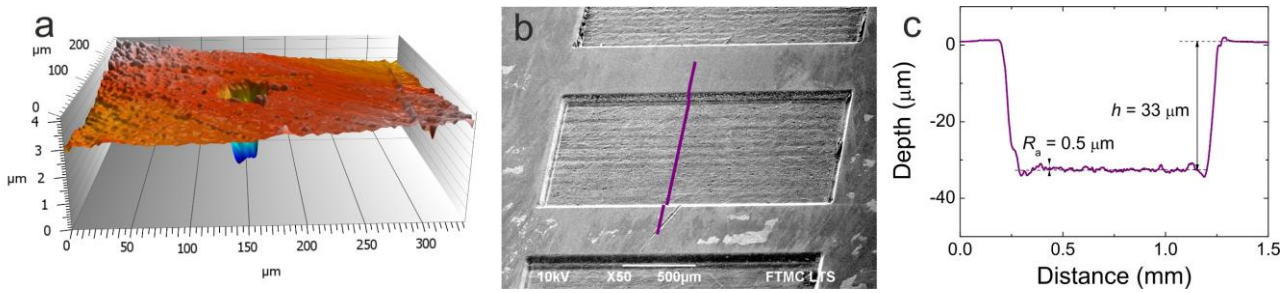

Fig. 3. Evaluation of laser ablation efficiency of processed copper. (a) Map of laser drilled crater measured by the optical 3D profiler, m = 10 pulses on one spot. (b) SEM image of laser milled cavity with (c) profile measured by the stylus profiler, n = 3 scans, scanning speed v =333 mm/s, hatch Δy = 10 µm. Pulse fluence F_0 = 3.3 J/cm^2, the laser wavelength λ = 1030 nm, pulse repetition rate f_P = 100 kHz, average optical power P_{ave} = 7.3 W.

2.3. Governing equations

Theoretically the ablation efficiency η_E dependence on laser pulse fluence F_0 is [8,9,17]:

$$\eta_{\mathrm{E}} = \frac{\delta}{2F_0} \ln^2\left(\frac{F_0}{F_{\mathrm{th}}}\right), \tag{5}$$

where δ – effective energy penetration depth, F_{th} – ablation threshold fluence, and F_0 – laser peak pulse fluence calculated by Equation (3). Since the ablation threshold F_{th} is beam width w dependent and w was varied during the experiments, the Equation (5) was improved by incorporating the extended defect model (EDM) [18,19]. EDM predicts F_{th} increase at small beam radius due to a lower possibility for the laser pulse to hit a defect within a smaller radius:

$$F_{\mathrm{th}}(w) = F_{\mathrm{d}} + (F_i - F_d)\left(\frac{F_{\mathrm{i}}}{F_{\mathrm{d}}}\right)^{-\frac{1}{2}w^2\pi\sigma}, \tag{6}$$

where F_d and F_i – low density defect mediated and intrinsic threshold fluencies, respectively and σ – real density of the optically active defects. Also, this model assumes that after a certain beam width w, the ablation threshold F_{th} is constant. The experimental data was fitted combining Equations (5) and (6):

$$\eta_{\mathrm{E}} = \frac{\delta}{2F_0} \ln^2\left(\frac{F_0}{F_{\mathrm{d}} + (F_i - F_d)\left(\frac{F_{\mathrm{i}}}{F_{\mathrm{d}}}\right)^{-\frac{\sigma E_p}{F_0}}}\right), \tag{7}$$

where $E_p = P_{ave}/(f_{P,B}NP)$ – is the energy of one pulse within the burst. Nevertheless, this model does not take into account the heat accumulation or plasma shielding which is usually present during high pulse repetition rate processing. Therefore, not all experimental data was successfully fitted by Equation (7). In this paper all the ablation efficiency versus pulse fluence graphs are either fitted by Equation (7) and depicted by solid lines or data points connected by straight dashed lines for eye guiding purposes.

2.4. Samples

Copper and stainless steel (1.4301) plates with dimensions of 50 × 50 × 5 mm^3 were used for laser ablation. Copper had a purity of 99.9% and surface roughness of R_a < 0.1 µm, while stainless steel surface roughness was R_a < 0.5 µm. For sample visualisation, scanning electron microscope (SEM) (JSM-6490LV, JEOL) was used. Copper and stainless steel were chosen as target materials due to high popularity in the theoretical and experimental studies of laser ablation process, which allows easier comparison of the results. Copper was used for laser drilling and milling experiments, stainless steel – for milling.

3. Results and discussion

3.1. MHz burst

The beam-size-optimisation method allows to simultaneously find the maximum ablation rate and the maximum ablation efficiency for a given set of laser processing parameters [9,20]. This optimisation method was applied for various pulse numbers per burst for drilling of craters and milling of rectangular cavities (see Methods section for the details). In the case of MHz burst processing of copper the strong dependence of odd and even number of pulses per burst was clearly visible for both crater ablation and cavity milling (Fig. 4). By using MHz burst the highest ablation efficiency for crater drilling was 8.8 $\mu m^3/\mu J$ for $N = 3$ pulses per burst and was higher than single-pulse regime efficiency by 15%. Also, $N = 5$ pulses per burst had a higher crater ablation efficiency by 12.5% compared to single-pulse regime. All other N values were less efficient than conventional single-pulse regime. For cavity milling the highest ablation efficiency was 5.6 $\mu m^3/\mu J$ for $N = 3$ pulses per burst and was higher than single-pulse regime efficiency by 8%. To the best of our knowledge, here we report the highest laser milling efficiency for copper material by ultrashort pulses at laser wavelength of ~1 µm. Similarly, the 3-pulses MHz burst processing was the most efficient regime for pulse-energy-optimisation [21] and beam-size-optimisation [7] for milling, but was never reported for drilling.

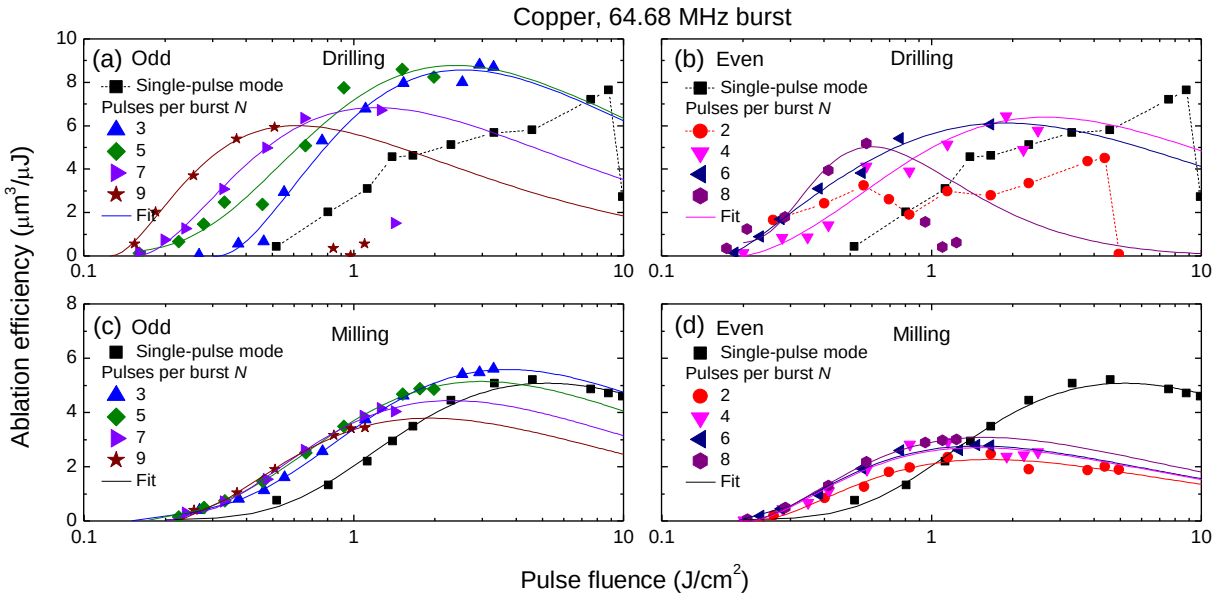

Fig. 4. Crater drilling and cavity milling efficiencies by MHz bursts for copper sample. (a, b) Crater drilling, (c, d) cavity milling. (a) and (c) data for odd number of pulses per burst N, (b) and (d) – even N values. Black squares are efficiencies for conventional single-pulse laser processing with pulse repetition rate of f_P = 100 kHz. The laser wavelength λ = 1030 nm, burst repetition rate f_B = 100 kHz, intra-burst repetition rate f_{MHz} = 64.68 MHz, average optical power P_{ave} = 7.3 W.

The clear ablation efficiency dependence on number of pulses per burst and processing approach is shown in Fig. 5 (c), where the maximum ablation efficiencies were extracted from Fig. 4. For both crater drilling and cavity milling two laser-initiated processes interchangeably play an important role: one responsible for the reduction of the ablation efficiency at even-pulses burst and the second – for the increase at odd-pulses burst. The process responsible for the reduction of the ablation efficiency is shielding of the second pulse by the plume of ablated particles [22] and plasma [23] produced by the first pulse. The second pulse hits the ablation cloud, the vaporisation of droplets and re-ignition of plasma starts. Due to the second pulse–ablation cloud interaction-induced pressure, part of the material from the ablation cloud might be forced to redeposit back on the target, as a consequence the shielding plume is dispersed [22]. The third pulse interacts with the target material pre-heated by the redeposited material and also does not suffer the plume attenuation. Therefore, the ablation efficiency is increased as hot material has a higher absorptance [21] and the energy required to raise the temperature to the boiling point of the pre-heated material is lower [24]. The higher volume of the material is ejected by the third pulse, which again creates the ablation plume and all the processes repeat again, resulting in periodical decrease-and-increase in ablation efficiency for the odd and even number of pulses per burst (Fig. 5 c). This triangle-wave-type dependency was material and intra-burst repetition rate dependent, since it was measured only for copper at MHz burst and biburst, but not for GHz burst (see later in Fig. 6 a and Fig. 8 a). Triangle-wave-type dependencies versus number of pulses per burst for copper crater drilling and cavity milling measured by two completely different processing approaches coincide perfectly, proving that the efficiency measurements are accurate and reliable. The curve of maximum ablation efficiency for drilling was shifted upwards by ~1.5 – 2 times depending on the number of pulses per burst, due to energetically more favourable approach of drilling. During the drilling process, in addition to the vaporisation, the molten material is expelled out of the crater in the state of liquid due to interaction-generated pressure, while milling approach is based on vaporisation only.

For the steel sample the influence of odd-pulses and even-pulses bursts on ablation efficiency was not observed (Fig. 5 a, b). The highest ablation efficiency was measured for the single-pulse processing mode and was 6.9 $\mu m^3/\mu J$. The MHz burst was more efficient than the single-pulse regime only for pulse fluence values higher than~2 J/cm^2. This can be explained by dense plasma/particle generation at high fluencies and the small spot sizes, which completely shield the laser beam. Therefore, the ablation efficiency close to ~0 $\mu m^3/\mu J$ was measured for single-pulse mode and pulse fluence near ~10 J/cm^2. The maximum ablation efficiency of steel dropped down by 35% for 2-pulses burst and 56% for 3-pulses burst compared with single-pulse processing (Fig. 5 d). For 4-pulses burst processing efficiency increased and stabilised at 5-pulses burst, but was still about 28% lower than single-pulse efficiency.

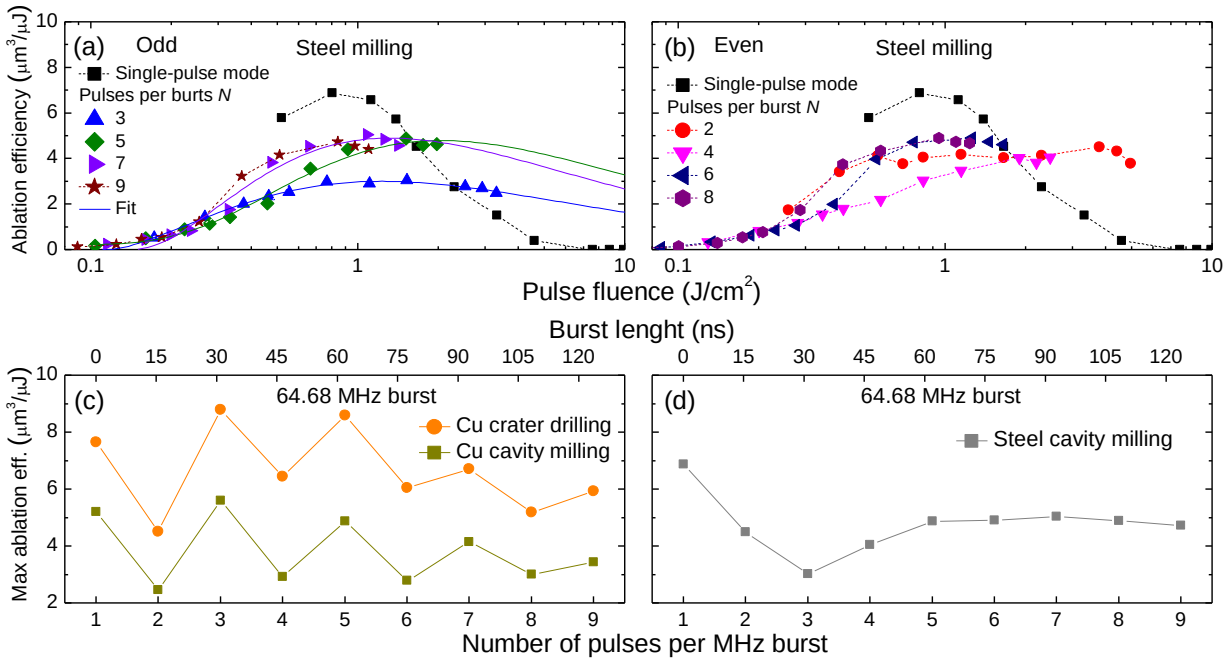

Fig. 5. Cavity milling efficiencies of MHz bursts for steel sample for (a) odd and (b) even number of pulses per MHz burst. Black squares are efficiencies for conventional single-pulse laser processing with pulse repetition rate of f_P = 100 kHz. (c) Maximum ablation efficiencies extracted from Fig. 4 versus number of pulses per MHz burst for drilling and milling of copper. (d) Maximum ablation efficiencies extracted from (a) and (b) versus number of pulses per MHz burst for milling of stainless steel. The laser wavelength λ = 1030 nm, burst repetition rate f_B = 100 kHz, intra-burst repetition rate f_{MHz} = 64.68 MHz, average optical power P_{ave} = 7.3 W.

3.2. GHz burst

The beam-size-optimisation was applied for GHz burst processing (Fig. 6). The ablation efficiency for copper milling decreased by 78% for P = 2 pulses burst and ~90% for P = 3 and up to P = 25 number of pulses per burst compared to single-pulse milling regime (Fig. 6 a). The similar ablation efficiency decrease was measured for steel milling: for P = 2-pulses burst efficiency decreased by 78%, for P = 3 and more pulses per burst – by 88% - 94% (Fig. 6 c). For GHz burst copper drilling the efficiency was also significantly reduced by 79% - 86% depending on the number of pulses per burst (Fig. 6 b). The maximum efficiency values were extracted from Fig. 6 (a) – (c) and plotted in Fig. 6 (d). The difference between copper drilling and milling was similar to the one measured for MHz burst – depending on the number of pulses per burst drilling was ~1.4 – 2.9 times more efficient than milling. The milling of copper and milling of steel had similar maximum ablation efficiency values versus number of pulses per burst, which proves that GHz burst processing is not metal material dependent, which was the case for MHz burst. The high efficiency decrease for GHz burst compared with single-pulse processing was due to the ultrafast laser-matter interaction induced plasma and particle shielding, which partially blocked the incoming laser pulses. In the case of 2-pulses burst processing,

205 ps distance between two pulses was not short enough to prevent attenuation of the second pulse by plasma/particles generated by the first pulse.

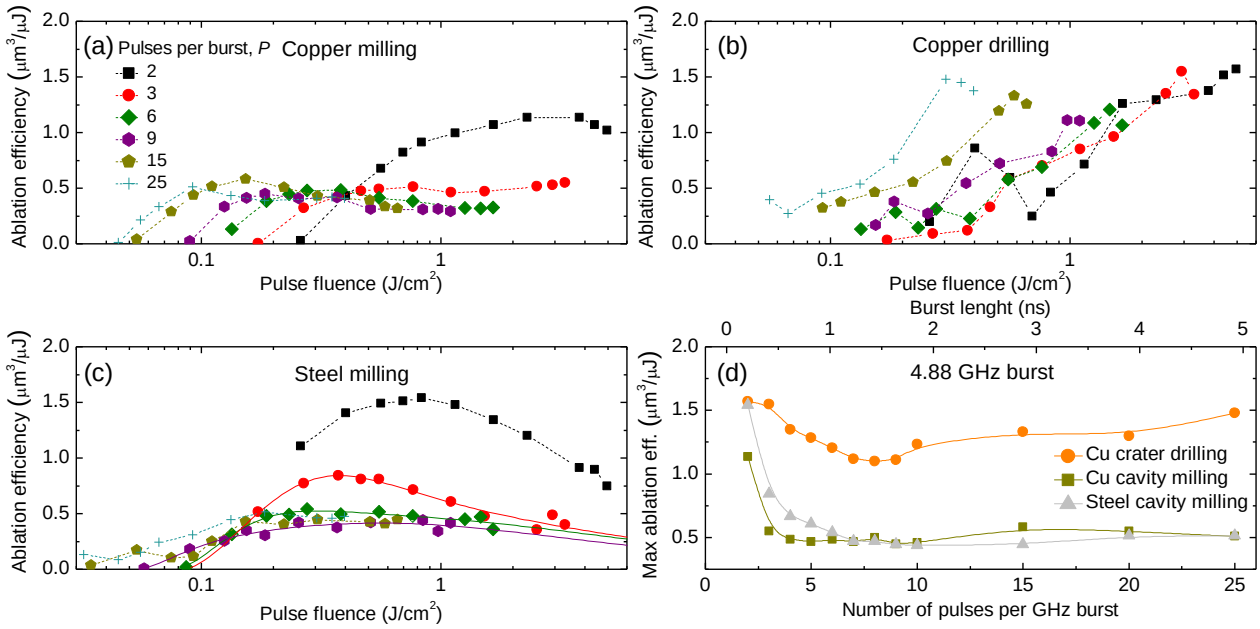

Fig. 6. Ablation efficiencies of GHz bursts for (a) copper cavity milling, (b) copper crater drilling and (c) steel cavity milling. (d) Maximum ablation efficiencies extracted from (a), (b), (c) versus number of pulses per MHz burst for milling and drilling of copper and milling of steel. The laser wavelength λ = 1030 nm, burst repetition rate f_B = 100 kHz, intra-burst repetition rate f_{GHz} = 4.88 GHz, average optical power P_{ave} = 7.3 W.

3.3. Biburst

The beam-size-optimisation was applied for biburst processing. Some of the measurement data are presented in Fig. 7, the rest of the data can be found in the supplementary material. In the case of copper and steel biburst milling the ablation efficiency values were not much different from the GHz burst milling being, at the best, about three times less efficient than single-pulse milling. The unexpected high ablation efficiency values were measured for copper biburst drilling, which at the certain number of pulses per burst combination, exceeded the value of the single-pulse drilling. Nevertheless, the MHz burst drilling was still more efficient than biburst drilling. The difference of biburst drilling and milling efficiencies was huge: for example, for the processing regime N = 5, P =25, copper drilling had the efficiency more than 12 times higher than milling (notice the ordinates values in Fig. 7 a and b). Similarly, the high difference between the efficiencies of milling and drilling of ~10 times was measured for 160-pulse 864 MHz burst and was explained by the different melt flow [12]. In the drilling procedure heat accumulation-induced melt is ejected out of the crater due to the recoil vapour pressure, while during the milling procedure, melt flows back on the previously processed area and does not contribute to the material removal.

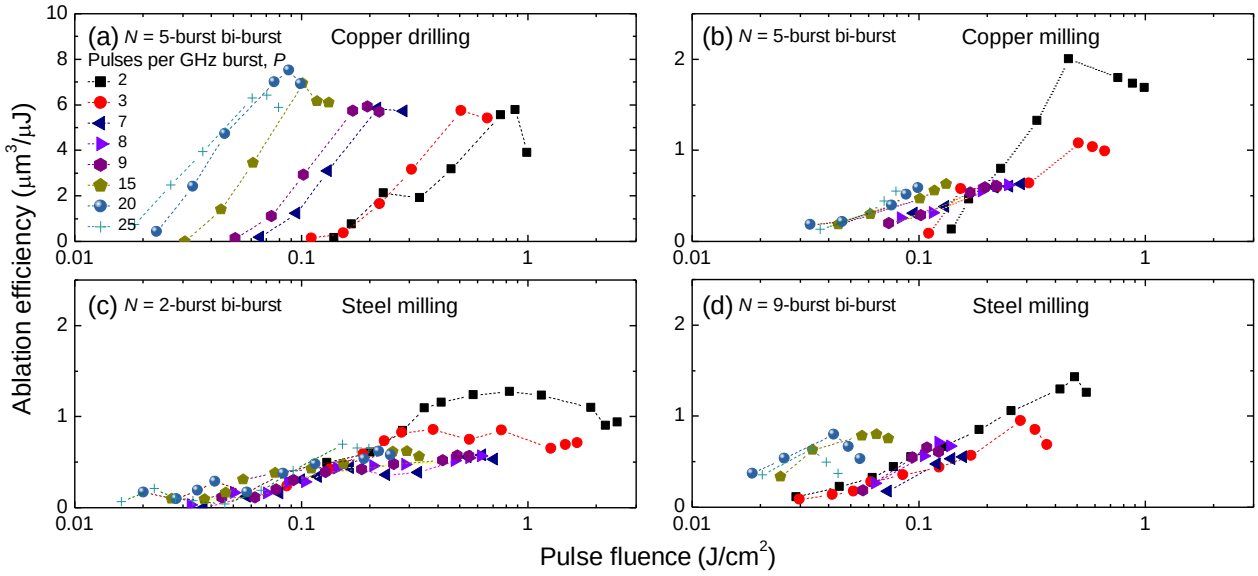

Fig. 7. Ablation efficiencies of biburst for (a) copper crater drilling by $N = 5$ bursts per biburst, (b) copper cavity milling by $N = 5$ bursts per biburst, (c) steel cavity milling by $N = 2$ bursts per biburst and (d) steel cavity milling by $N = 9$ bursts per biburst. The laser wavelength $\lambda = 1030$ nm, biburst repetition rate $f_B = 100$ kHz, burst repetition rate $f_{MHz} = 64.68$ MHz, pulse repetition rate $f_{GHz} = 4.88$ GHz, average optical power $P_{ave} = 7.3$ W.

The maximum ablation efficiency values were extracted from all the measured ablation efficiency versus pulse fluence graphs (Fig. 8). In the case of copper milling by biburst, the influence of odd and even number of bursts per biburst N was evident only for $P = 2$ pulses per GHz burst (Fig. 8 a). This triangle-type-wave dependence was similar to the one measured for the MHz burst processing (Fig. 5 c). Contrary, the biburst copper drilling did not have the same shape as MHz burst drilling (Fig. 8 b). The drop of ablation efficiency was not measured for $N = 4$ bursts per biburst, ruining the triangle-type-wave graph as was the case for MHz burst processing. The reason for this cannot be explained yet. For steel biburst milling the small influence of number of bursts per biburst N for maximum ablation efficiency was measured (Fig. 8 c). The highest ablation efficiencies achieved in this work for each of the processing mode and approach are summarised in Fig. 8 (d). SEM images and profiles of the most efficient drilling and milling regimes together with surface roughness are presented in Fig. 9. As shown in our previous works, the ablation efficiency optimisation via beam size [7,20] and pulse energy [25] also results in high-quality. The smallest surface roughness achieved in this work for cavity milling was as low as $R_a = 0.1$ µm showing the promising utilisation of ultrafast bursts in the polishing [26] and high-quality surface treatment [27] applications.

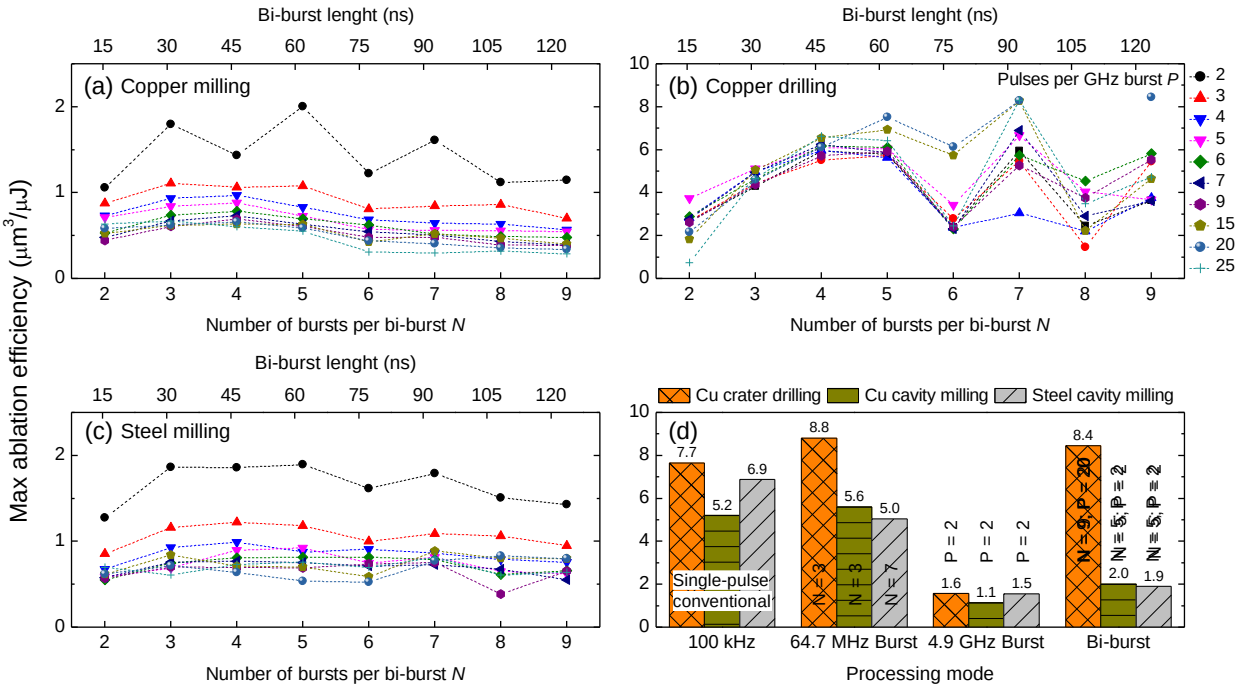

Fig. 8. Maximum ablation efficiencies for biburst (a) copper milling, (b) copper drilling and (c) steel milling. (d) The highest ablation efficiencies of drilling and milling measured for four different processing modes. The laser wavelength λ = 1030 nm, burst repetition rate f_{MHz} = 64.68 MHz, pulse repetition rate f_{GHz} = 4.88 GHz, average optical power P_{ave} = 7.3 W.

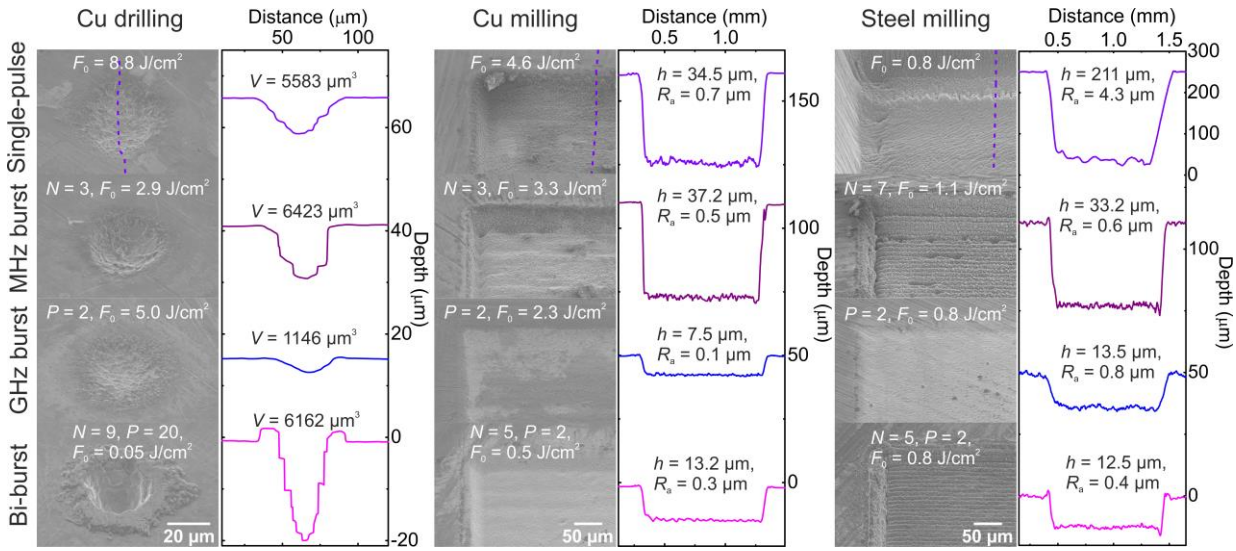

Fig. 9. SEM images and profiles of the most efficient drilling and milling regimes for various processing modes. V – volume of the crater, h – depth of the cavity, R_a – surface roughness, F_0 – pulse fluence, N and P – number of pulses per MHz and GHz burst, respectively. The laser wavelength λ = 1030 nm, repetition rate $f_{P,B}$ = 100 kHz, intra-burst repetition rates f_{MHz} = 64.68 MHz and f_{GHZ} = 4.88 GHz, average optical power P_{ave} = 7.3 W.

Overall, the highest ablation efficiency values for copper were measured for MHz burst processing and N =3 pulses per burst and was 8.8 μm³/μJ for drilling and 5.6 μm³/μJ for milling, while the steel milling efficiency was highest for conventional single-pulse regime with 6.9 μm³/μJ. Even though, the biburst processing did

not show the highest ablation efficiencies among other processing modes, to the best of our knowledge, in this work we achieved the highest ever published efficiency values for ultrashort pulses at ~1 µm wavelength. The previous highest ablation efficiency values were 7.6 $\mu m^3/\mu J$ [6] for copper drilling, 4.8 $\mu m^3/\mu J$ [7] for copper milling and 4.1 $\mu m^3/\mu J$ [28] for steel milling. For more information about the processing parameters utilised in other studies and typical efficiency values see Table 1.

Table 1. Typical ablation efficiency values reported in the literature. f_P – intra-burst repetition rate, N – number of pulses per burst, λ – laser wavelength, τ_p – pulse duration, w_0 – beam radius, f – pulse or burst repetition rate, v – beam scanning speed, Δy – hatch distance.

	Copper				**Stainless steel**	
	Drilling ($\mu m^3/\mu J$)	f_P, N, λ, τ_p, w_0, f	***Milling*** ($\mu m^3/\mu J$)	f_P, N, λ, τ_p, w_0, f, v, Δy	***Milling*** ($\mu m^3/\mu J$)	f_B, N, λ, τ_p, w_0, f, v, Δy
Burst	**7.6** [6]	3.456 GHz, 800 ppb, 1035 nm, 1 ps, 12 µm, 1 kHz	**2.6** [29]	83 MHz, 3 ppb, 1064 nm, 10 ps, 16 µm, 200 kHz, 1.6 m/s, 8 µm	**2.3** [29]	83 MHz, 3 ppb, 1064 nm, 10 ps, 16 µm, 200 kHz, 1.6 m/s, 8 µm
	6.5 [30]	1.6 GHz, 400 ppb, 1050 nm, 300 fs, 11.5 µm, 200 kHz	**4.2** [28]	148 MHz, 28 ppb, 1040 nm, 380 fs, 9 µm, 100 kHz, 750 mm/s, 7.5 µm	**2.5** [28]	148 MHz, 28 ppb, 1040 nm, 380 fs, 9 µm, 100 kHz, 750 mm/s, 7.5 µm
	8.8 [This work]	64.68 MHz, 3 ppb, 1030 nm, 210 fs, 23 µm, 100 kHz	**5.6** [This work]	64.68 MHz, 3 ppb, 1030 nm, 210 fs, 21.7 µm, 100 kHz, 300 mm/s, 10 µm	**5.0** [This work]	64.68 MHz, 7 ppb, 1030 nm, 210 fs, 24.8 µm, 100 kHz
Single-pulse	**0.7** [10]	-, -, 1064 nm, 10 ps, 10 µm, 100 kHz	**2.22** [29]	-, -, 1064 nm, 10 ps, 16 µm, 200 kHz – 1.6 MHz, 8 µm	**2.25** [29]	-, -, 1064 nm, 10 ps, 16 µm, 200 kHz – 1.6 MHz, 8 µm
	1.9 [31]	-, -, 1064 nm, 10 ps, 31.45 µm, 50 Hz	**3.1** [28]	-, -, 1040 nm, 380 fs, 9 µm, 100 kHz, 750 mm/s, 7.5 µm	**4.1** [28]	-, -, 1040 nm, 380 fs, 9 µm, 100 kHz, 750 mm/s, 7.5 µm
	7.7 [This work]	-, -, 1030 nm, 210 fs, 23 µm, 100 kHz	**5.2** [This work]	-, -, 1030 nm, 210 fs, 31.8 µm, 100 kHz, 300 mm/s, 10 µm	**6.9** [This work]	-, -, 1030 nm, 210 fs, 76 µm, 100 kHz, 300 mm/s, 10 µm

4. Conclusions

The in-depth study of maximum ultrafast laser ablation efficiency for processing of copper and steel by single-pulses, MHz-, GHz- and biburst was performed. In the case of copper MHz burst milling and drilling the ablation efficiency was highly depended on odd and even number of pulses per burst. The MHz burst drilling was up to two times more efficient than milling process with the same triangle-type-wave dependence on number of pulses per burst. This type dependence was material dependent. Steel MHz burst milling had a completely different tendency with no evidence of odd and even number of pulses per burst influence on

the ablation efficiency. The GHz processing revealed to be highly inefficient for both milling and drilling and for both copper and steel compared to single-pulse processing. For the first time the biburst mode processing, consisting of GHz bursts inside of MHz bursts, was used for the materials processing. The biburst milling of copper and steel did not improve the ablation efficiency compared to the single-pulse milling. The biburst drilling efficiency of copper had the higher ablation efficiency than the single-pulse drilling. In this paper we report 3 high efficiency ablation values for ultrashort pulse laser processing at ~1 µm wavelength: 8.8 $\mu m^3/\mu J$ (0.5 mm^3/min/W) for copper drilling, 5.6 $\mu m^3/\mu J$ (0.3 mm^3/min/W) for copper milling and 6.9 $\mu m^3/\mu J$ (0.4 mm^3/min/W) for steel milling.

CRediT authorship contribution statement

Andrius Žemaitis: Conceptualization, Methodology, Validation, Investigation, Visualization, Writing - Original Draft. **Mantas Gaidys**: Investigation, Formal analysis. **Paulius Gečys**: Resources, Funding acquisition. **Martynas Barkauskas**: Resources. **Mindaugas Gedvilas**: Funding acquisition, Supervision.

Declaration of Competing Interest

The authors declare that they have no known competing financial interests or personal relationships that could have appeared to influence the work reported in this paper.

Acknowledgement

Funding from Research Council of Lithuania (LMT) (01.2.2-LMT-K-718-03-0050).

References

[1] Y. Liu, J. Wu, X. Wen, W. Lin, W. Wang, X. Guan, T. Qiao, Y. Guo, W. Wang, X. Wei, Z. Yang, >100 W GHz femtosecond burst mode all-fiber laser system at 1.0 µm, Opt. Express. 28 (2020) 13414–13422. doi:10.1364/OE.391515.

[2] J. Mur, R. Petkovšek, Near-THz bursts of pulses – Governing surface ablation mechanisms for laser material processing, Appl. Surf. Sci. 478 (2019) 355–360. doi:https://doi.org/10.1016/j.apsusc.2019.01.182.

[3] U. Loeschner, J. Schille, A. Streek, T. Knebel, L. Hartwig, R. Hillmann, C. Endisch, High-rate laser microprocessing using a polygon scanner system, J. Laser Appl. 27 (2015) S29303. doi:10.2351/1.4906473.

[4] R. Weber, T. Graf, P. Berger, V. Onuseit, M. Wiedenmann, C. Freitag, A. Feuer, Heat accumulation during pulsed laser materials processing, Opt. Express. 22 (2014) 11312–11324. doi:10.1364/OE.22.011312.

[5] F. Bauer, A. Michalowski, T. Kiedrowski, S. Nolte, Heat accumulation in ultra-short pulsed scanning laser ablation of metals, Opt. Express. 23 (2015) 1035–1043. doi:10.1364/OE.23.001035.

[6] C. Kerse, H. Kalaycıoğlu, P. Elahi, B. Çetin, D.K. Kesim, Ö. Akçaalan, S. Yavaş, M.D. Aşık, Ö. Bülent, H. Heinar, H. Ronald, F.Ö. Ilday, Ablation-cooled material removal with ultrafast bursts of pulses, Nature. 537 (2016) 84–88. doi:10.1038/nature18619.

[7] A. Žemaitis, P. Gečys, M. Barkauskas, G. Račiukaitis, M. Gedvilas, Highly-efficient laser ablation of copper by bursts of ultrashort tuneable (fs-ps) pulses, Sci. Rep. 9 (2019) 12280. doi:s41598-019-48779-w.

[8] J. Furmanski, A.M. Rubenchik, M.D. Shirk, B.C. Stuart, Deterministic processing of alumina with ultrashort laser pulses, J. Appl. Phys. 102 (2007) 073112. doi:10.1063/1.2794376.

[9] G. Račiukaitis, M. Brikas, P. Gečys, B. Voisiat, M. Gedvilas, Use of High Repetition Rate and High Power Lasers in Microfabrication: How to Keep the Efficiency High?, J. Laser Micro Nanoen. 4 (2009) 186–191. doi:10.2961/jlmn.2009.03.0008.

[10] W. Hu, Y.C. Shin, G. King, Modeling of multi-burst mode pico-second laser ablation for improved material removal rate, Appl. Phys. A. 98 (2010) 407–415. doi:10.1007/s00339-009-5405-x.

[11] M.E. Povarnitsyn, P.R. Levashov, D. V Knyazev, Simulation of ultrafast bursts of subpicosecond pulses: In pursuit of efficiency, Appl. Phys. Lett. 112 (2018) 51603. doi:10.1063/1.5012758.

[12] H. Matsumoto, Z. Lin, J. Kleinert, Ultrafast laser ablation of copper with ~GHz bursts, Proc. SPIE. 10519 (2018) 1051902. doi:10.1117/12.2294041.

[13] D. Metzner, P. Lickschat, S. Weißmantel, Influence of heat accumulation during laser micromachining of CoCrMo alloy with ultrashort pulses in burst mode, Appl. Phys. A. 126 (2020) 84. doi:10.1007/s00339-019-3203-7.

[14] J.M. Liu, Simple technique for measurements of pulsed Gaussian-beam spot sizes, Opt. Lett. 7 (1982) 196–198. doi:10.1364/OL.7.000196.

[15] H. Sun, Thin lens equation for a real laser beam with weak lens aperture truncation, Opt. Eng. 37 (1998) 2906–2913. doi:10.1117/1.601877.

[16] A. Žemaitis, M. Gaidys, M. Brikas, P. Gečys, G. Račiukaitis, M. Gedvilas, Advanced laser scanning for highly-efficient ablation and ultrafast surface structuring: experiment and model, Sci. Rep. 8 (2018). doi:10.1038/s41598-018-35604-z.

[17] B. Neuenschwander, G.F. Bucher, C. Nussbaum, B. Joss, M. Muralt, U.W. Hunziker, P. Schuetz, Processing of metals and dielectric materials with ps-laser pulses: results, strategies, limitations and needs, Laser Appl. Microelectron. Optoelectron. Manuf. 7584 (2010) 75840R. doi:10.1117/12.846521.

[18] O. Armbruster, A. Naghilou, M. Kitzler, W. Kautek, Spot size and pulse number dependence of femtosecond laser ablation thresholds of silicon and stainless steel, Appl. Surf. Sci. 396 (2017) 1736–1740. doi:10.1016/j.apsusc.2016.11.229.

[19] A. Naghilou, O. Armbruster, W. Kautek, Femto- and nanosecond pulse laser ablation dependence on irradiation area: The role of defects in metals and semiconductors, Appl. Surf. Sci. 418 (2017) 487–490. doi:10.1016/j.apsusc.2016.12.141.

[20] A. Žemaitis, M. Gaidys, P. Gečys, G. Račiukaitis, M. Gedvilas, Rapid high-quality 3D micro-machining by optimised efficient ultrashort laser ablation, Opt. Lasers Eng. 114 (2019) 83–89. doi:10.1016/j.optlaseng.2018.11.001.

[21] B. Jäggi, D.J. Förster, R. Weber, B. Neuenschwander, Residual heat during laser ablation of metals with bursts of ultra-short pulses, Adv. Opt. Technol. 7 (2018) 175–182. doi:10.1515/aot-2018-0003.

[22] D.J. Förster, S. Faas, S. Gröninger, F. Bauer, A. Michalowski, R. Weber, T. Graf, Shielding effects and re-deposition of material during processing of metals with bursts of ultra-short laser pulses, Appl. Surf. Sci. 440 (2018) 926–931. doi:10.1016/j.apsusc.2018.01.297.

[23] J. König, S. Nolte, A. Tünnermann, Plasma evolution during metal ablation with ultrashort laser pulses., Opt. Express. 13 (2005) 10597–10607. doi:10.1364/OPEX.13.010597.

[24] A. Žemaitis, J. Mikšys, M. Gaidys, P. Gečys, M. Gedvilas, High-efficiency laser fabrication of drag reducing riblet surfaces on pre-heated Teflon, Mater. Res. Express. 6 (2019) 065309. doi:10.1088/2053-1591/ab0b12.

[25] M. Gaidys, A. Žemaitis, P. Gečys, M. Gedvilas, Efficient picosecond laser ablation of copper cylinders, Appl. Surf. Sci. 483 (2019). doi:10.1016/j.apsusc.2019.04.002.

[26] A. Brenner, M. Zecherle, S. Verpoort, K. Schuster, C. Schnitzler, M. Kogel-Hollacher, M. Reisacher, B. Nohn, Efficient production of design textures on large-format 3D mold tools, J. Laser Appl. 32 (2020) 12018. doi:10.2351/1.5132401.

[27] D. Metzner, P. Lickschat, S. Weißmantel, High-quality surface treatment using GHz burst mode with tunable ultrashort pulses, Appl. Surf. Sci. 531 (2020) 147270. doi:https://doi.org/10.1016/j.apsusc.2020.147270.

[28] M. Domke, V. Matylitsky, S. Stroj, Surface ablation efficiency and quality of fs lasers in single-pulse mode, fs lasers in burst mode, and ns lasers, Appl. Surf. Sci. 505 (2020) 144594. doi:https://doi.org/10.1016/j.apsusc.2019.144594.

[29] T. Kramer, Y. Zhang, S. Remund, B. Jaeggi, A. Michalowski, L. Grad, B. Neuenschwander, Increasing the Specific Removal Rate for Ultra Short Pulsed Laser-Micromachining by Using Pulse Bursts, J. Laser Micro Nanoen. 12 (2017) 107–114. doi:10.2961/jlmn.2017.02.0011.

[30] Pa. Elahi, Ö. Akçaalan, C. Ertek, K. Eken, F.Ö. Ilday, H. Kalaycoglu, High-power Yb-based all-fiber laser delivering 300 fs pulses for high-speed ablation-cooled material removal, Opt. Lett. 43 (2018) 535–538.

[31] B. Lauer, B. Jaeggi, Y. Zhang, B. Neuenschwander, Measurement of the Maximum Specific Removal Rate: Unexpected Influence of the Experimental Method and the Spot Size (M701), Int. Congr. Appl. Lasers Electro-Optics. (2015) 146–154. http://icaleo2015.conferencespot.org/59277lia-1.2681067/t002-1.2681865/f004-1.2681881/a009-1.2681891/ap035-1.2681898.